

## NUMERICAL SIMULATION OF FAILURE PROCESS ON CONCRETE-FILLED STEEL TUBE UNDER ECCENTRIC COMPRESSION

G.P.ZOU<sup>\*</sup>, Z.L.CHANG<sup>\*</sup>, X.D.ZHANG<sup>†</sup>, D.WANG<sup>\*</sup>, J.LIN<sup>\*</sup>, X.H.SHEN<sup>\*</sup>

<sup>\*</sup> Harbin Engineering University, School of Aerospace and Civil Engineering, Harbin 150001, China  
E-mail: gpzou@hotmail.com

<sup>†</sup> Inner-Mongolia Power Exploration & Design Institute, Inner-Mongolia 010020, China

**Key words:** Concrete-filled rectangular steel tube; Numerical simulation; Failure process, Eccentric compression

**Abstract:** Concrete-filled steel tube is a new kind of building material, in this structure, the steel pipe is utilized to constraint its core concrete and make the core concrete under complex stress state, so the concrete strength can be improved, its ductility and toughness can be improved too. This structure possesses high bearing load capacity, good ductility, good anti-seismic performance, fire resistance property and low cost. It has been widely used in the civil engineering, such as bridge structures, high-rise buildings, and industrial plants and so on. Now the concrete-filled steel tube has been studied a lot and have made great progress, however, for its eccentric compression performance study is little, this may cause by the concrete filled steel tube possess good bearing capacity, and eccentric compression loading is very difficult to realized, however the concrete columns which under eccentric compression is a common form of engineering structures, so it is necessary to study the failure and damage process of concrete-filled steel tube under eccentric compression load. In this paper, the Realistic Failure Process Analysis (RFPA<sup>3D</sup>) software was used to simulate the concrete-filled rectangular steel tube which is subjected to axial and eccentric compression load. Through simulate the real experimental of concrete-filled steel tube under axial compression, we can get the correct simulation parameter, and then utilize these parameters to study the concrete-filled steel tube under eccentric compression. From the simulation we can obtained the stress distribution and damage during the whole loading process until the concrete-filled steel tube failure, and also study the eccentric ratio influence to crack expending and structure failure phenomenon, and this study can be provide good reference for the application of concrete-filled steel tube.

### 1 INTRODUCTION

Concrete-filled steel tube, as a kind of new building material, it is widely used in many civil engineering projects (such as bridge structures, high-rise buildings and industrial buildings). The researches and applications of the concrete-filled circular and square steel tube have been getting more attention in China, but the studies about the fracture and failure mechanism of the concrete-filled rectangular steel tube are not profoundly enough, where

the further investigations are still needed<sup>[1-3]</sup>. Numerical simulation software-RFPA<sup>3D</sup> can be used simulating the damage process of brittle material (such as rock and concrete), and it has been successfully used in simulating the fracture process of rock and concrete<sup>[4-6]</sup>. Therefore, the paper carries on the numerical simulation on the damage process of concrete-filled rectangular steel tube by RFPA<sup>3D</sup>. First, in order to get correct parameters on simulation, the RFPA<sup>3D</sup> was used to simulating

the real concrete-filled rectangular steel tube axial compression experiment, compare the ultimate bearing capacity and load-strain curve of concrete-filled steel tube with experiment data in paper [7], simulation data can match with test data well, then the correct simulation parameters is obtained. And then use these parameters to simulate the eccentric compression of concrete-filled steel tube, through simulate calculation, it can be got the cracks growth process, reappeared the concrete-filled steel tube failure process which under eccentric compression, through the simulation results we can canvassed study the failure mechanism of concrete-filled rectangular steel tube column which under axial and eccentric compression.

## 2 AXIAL COMPRESSIVE NUMERICAL SIMULATION STUDY OF CONCRETE-FILLED STEEL TUBE BASED ON THE RFPA<sup>3D</sup> SOFTWARE

### 2.1 Concrete-filled steel tube compression experiment

Concrete-filled steel tube compression experiment was shown in paper [7], the specimen cross-section as shown in fig.1,  $D$  is the cross-section length of specimen;  $B$  is the cross-section width of specimen;  $t$  is the thickness of steel tube wall. Fig.2 is schematic diagram of the experiment, the experiment was done by 200T compression-testing machine, in order to test the strain of the specimen under compression, in the middle length of the specimen, the strain gage was pasted on the lateral direction and axial direction, and install two tensiometer along the specimen length to test the total deformation, as shown in fig.2, and  $L$  is the original length of specimen. In the experiment  $L/D=3$ .

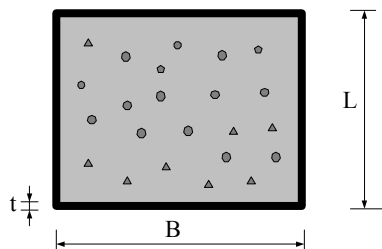


Figure 1 Concrete-filled steel tube

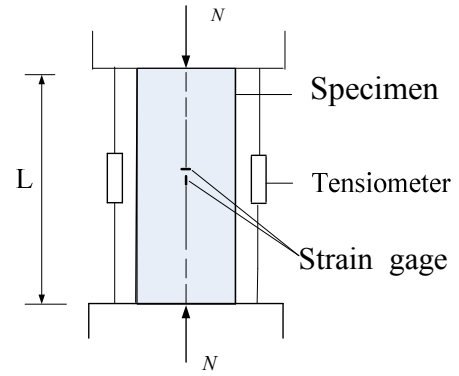


Figure 2 Schematic diagram of the compress experiment

The stepped loading mode was adopted to compress the specimen, during the elastic stage, every step load value was the 1/10 of anticipate ultimate load value, when reach yielding stage, every step load value was the 1/15 of anticipate ultimate load value, every step load sustain 2~3 minutes, the slow continuous loading was adopted when the specimen was close to destruction. The strain and displacement data was automatic collected by computer acquisition system.

Through observe the experiment, the concrete-filled steel tube possess good ductile ability and good bearing capacity. In the initial loading stage, there is little shape deformation, when load reach the 60% to 70% of ultimate load, the steel tube local part will appear shear glide lines, as the load increasing, the shear glide lines are increasing, when appear all the steel tube surface, and the specimen will be broken.

### 2.2 Numerical simulation model

The specimen model and test results which is adopted in this paper is according to the reference paper [7]. Considering the character of the RFPA<sup>3D</sup>, the specimen should be divided into several cubic elements for calculating. The sizes of numerical simulation are shown in Table 1.

Table 1 The sizes of numerical simulation

Specimen No.	$D \times B \times t$ (mm)	$L$ (mm)	$D/B$
Mc6	$100.1 \times 74.36 \times 2.86$	300.3	1.3

The mechanical parameters of concrete and steel tube are random valued by RFPA<sup>3D</sup> while their homogeneous degree and mean value are given. The parameter of concrete as follows: homogeneous degree is 3; elastic modulus of concrete is 44.6GPa; uniaxial compressive strength is 126Mpa; poisson ratio is 0.18; tension-compression ratio is 10; residual strength coefficient is 0.4. The ideal elastic-plastic model are adopted to simulate the steel tube. Its homogeneous degree is 200; poisson ratio is 0.3; the dimension parameters the same with document[7]. Considering the concrete properties of tensile failure and shear failure, the mohr-coulomb strength criterion is adopted, internal friction angle is  $30^0$ , and the step-by-step displacement control is adopted in the numerical simulation loading.

### 2.3 Results analyzed by numerical simulation

The ultimate bearing capacity which was tested from experiments in reference [7] and the ultimate bearing capacity which obtained by numerical simulation was showed in Table 2. From Table 2, it can be seen that the experiment results and numerical simulation results are very close.

**Table 2** Ultimate bearing capacity value of the experiments and numerical simulation

Experiment		Numerical simulation	
Specimen No.	Load (KN)	Specimen No.	Load (KN)
Mc6-1	640	Mc6	640
Mc6-2	672		

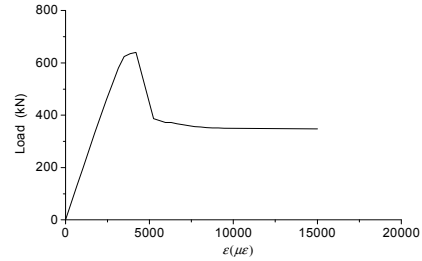
The experiment and simulation results of load-longitudinal strain curves as shown in fig.3, the curve can be divided into 4 stages:

Elastic stage: in this state, both of the tube and the core concrete are always independent bearing.

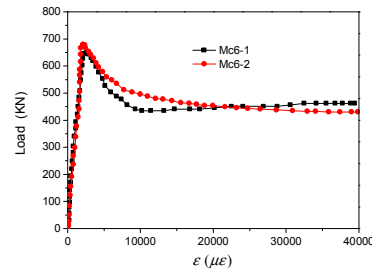
Elastic-plastic stage: the micro cracks of the core concrete under the longitudinal pressure would be unfolded continuously. When the coefficient of lateral deformation surpasses the poisson ratio, the deformation would be restricted by the steel tube.

Descending stage: load-longitudinal strain curve would be descending after got the peak value. In this stage, load falls rapidly as the development of the deformation.

Flat stage: the deformation of the load-strain relation develops quickly, but the descending amplitude of load is little.



(a) Load-strain curve obtain from numerical simulation



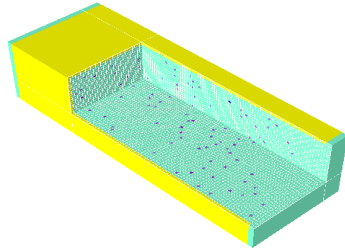
(b) Load-strain curve obtain from reference paper[7]

**Figure 3:** Mc6 Simulation and experimental curve.

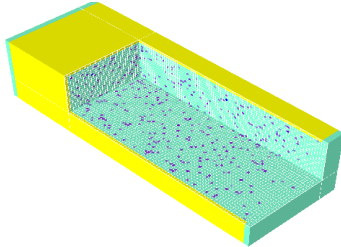
### 2.4 Analysis of fracture process

The numerical simulation results of the internal destructive process of specimen MC6 is shown in figure 4. From fig.4 it can be seen, under the 8th step of loading, there are a few elements of concrete begin to be broken. In the 11th step of loading, the destructive elements of concrete increase, the load doesn't reach its ultimate. When it gets the 14th step, high-stress areas concentrate in the interface of tube and concrete and the bond action between steel tube and concrete degraded gradually. In the 17th step of loading, many micro cracks in the concrete propagate rapidly which form transverse cracks. Local steel tube is on buckling and cylinder surface begin to bulge. Because of the constraint of steel tube, the extensions of cracks in the concrete are delayed effectively. When the loading gets the 32nd step, the buckling phenomena of steel

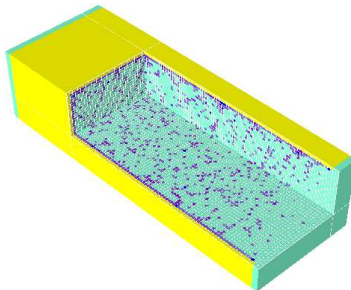
tube become obvious. The broken elements of concrete multiply with squeeze flow simultaneously. The deformation starts to develop fast. After that, the damaged elements of concrete begin to coalesce and form the large damage area as the displacement increase. The tube as above deforms outside, and the specimen shorten inch by inch. The damage area enlarges while the load-strain curve extends gradually.



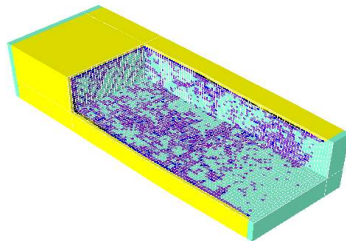
Step 8



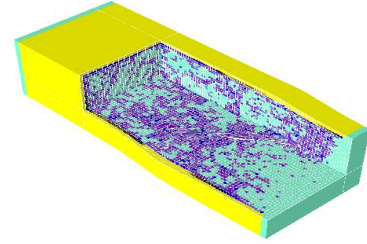
Step 11



Step 14



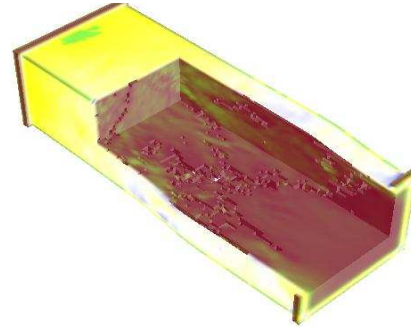
Step 17



Step 32

**Figure 4:** Failure process of specimen MC6.

Fig.5 is the graph of expansion cracks in the concrete-filled steel tube. It shows that the area cracks initiate densely and the place the steel tube where is on buckling accord. The steel tube restricts the concrete well.

**Figure 5:** Graph of expansion cracks.

### 3 ECCENTRIC COMPRESSION NUMERICAL EXPERIMENT OF CONCRETE-FILLED RECTANGULAR STEEL TUBE

#### 3.1 Establishing of the testing model

When calculating the compressive capacity which is perpendicular to plane where the moment is on for the internal column of multistoried building and baroclinic web member of roof truss which absorbs the dead loading, we can neglect the moment because of its minute in engineering. Therefore, the small eccentric compressions of columns always result from errors and dimension deviations of beams and columns among the construction process, and most of large ones form because of non-complete lapping of beams and columns. Additionally, a majority of beam and column nodes in the concrete-filled steel tube are rigidity nodes, for that reason, we assume that as Fig.6 shown, for studying the damage character of concrete-

filled rectangular steel tube:

On the section of beam and column lapping, this portion maintains level with load at the same time when deforming because of rigid connection. The others sections are free and column bottom is fixed. On the lapping section, the displacement load is applied well-proportioned to assure the synchronous deformation of faying surface. The model will study by the numerical simulation analysis in the rest of research.

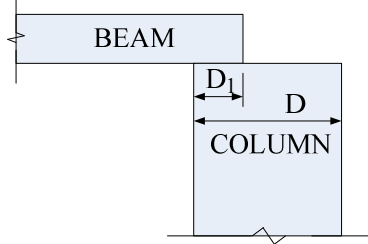


Figure 6: Construction diagram of model.

### 3.2 Selection of testing model parameter

In the failure process of analyzing axially loaded short columns, specimen Mc6 is used for simulation. Therefore, the numerical model size is the same as Table 1.

The beam lap length is  $D_1$ , and the cross-section length of specimen is  $D$ , as shown in fig6. In the numerical simulation the value  $D_1/D$  is  $1/4$ ,  $1/2$  and  $3/4$ . In order to guarantee the well-distributed loading of lapping section, a rigid cover board is added on the overlapping part section, and other numerical simulation parameters are same with before.

### 3.3 Analyzing the results of numerical test

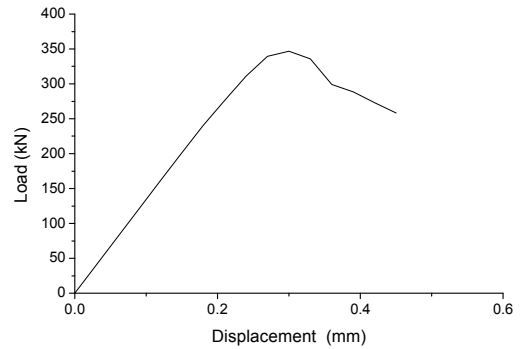
#### 3.3.1 Analyzing results

Table 3 is the numerical simulation results. It is obvious that there is no proportion relationship between the ultimate load and eccentric ratio.

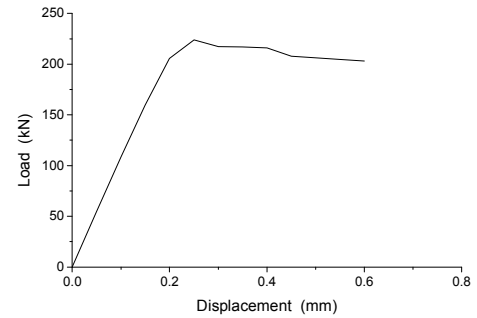
Table 3 Numerical simulation results

$D_1/D$	1	3/4	1/2	1/4
Max Loads(KN)	640	347	216	156
Compare with axial compression	100%	54%	34%	25%

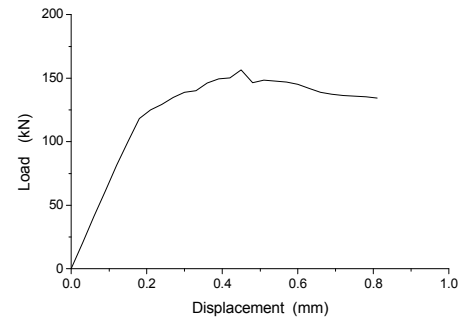
Fig. 7 is the force-displacement curve of the specimen. According to the curve results, under this loading mode, it would not descend suddenly after the concrete-filled rectangular steel tube climaxes the ultimate load. With the increase of eccentric ratio, the curve is more gentle. The ultimate load of non-complete lapping concrete-filled rectangular steel tube column is not as high as the concrete-filled steel tube under axial pressure, however, it didn't exist descending stage, so the structure will didn't abruptly collapse when under the ultimate load.



(a)  $D_1/D = 3/4$



(b)  $D_1/D = 1/2$



(c)  $D_1/D = 1/4$

Figure 7: Stress-displacement curve.



### 3.3.2 Process analysis of structure failure

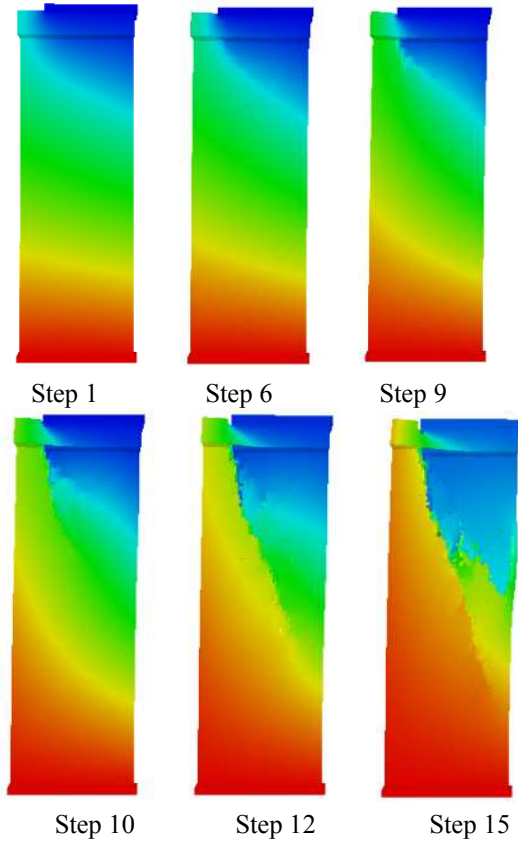


Figure 8: Failure process of  $D_1/D = 3/4$ .

Fig. 8 are several important loading steps of Mc6 concrete filled steel tube for 3/4 lap length during whole failure process, we can see:

Under loading, the maximum stress distribute in a triangular area; With the load carried, column become shorter obviously, and the concrete under the junction of lapped surface and free surface begin to destroy. Increasing loading time, the destroyed concrete begin to form crack, and the steel tube has the phenomenon of lateral bending; the 10<sup>th</sup> step, the crack continues to expand, and the steel tube starts to be torn on the junction of the lapped surface and free surface, at the same time, the load has reached the maximum. Step 12, new crack has been generated in the concrete, the lapped surface has lateral displacement with development of the cracks. And the original crack goes on expanding; Increasing load, the place where steel tube torn expands, cracks coalescence, the portion which is made of cracks and the

part under the lapped surface forms a lateral zone. Near the new crack bottom, steel tube wall buckles outward and protrudes. A gap occurs between steel tube and concrete.

In the whole process, although the steel tube has the overall lateral bending phenomenon, it is not obvious.

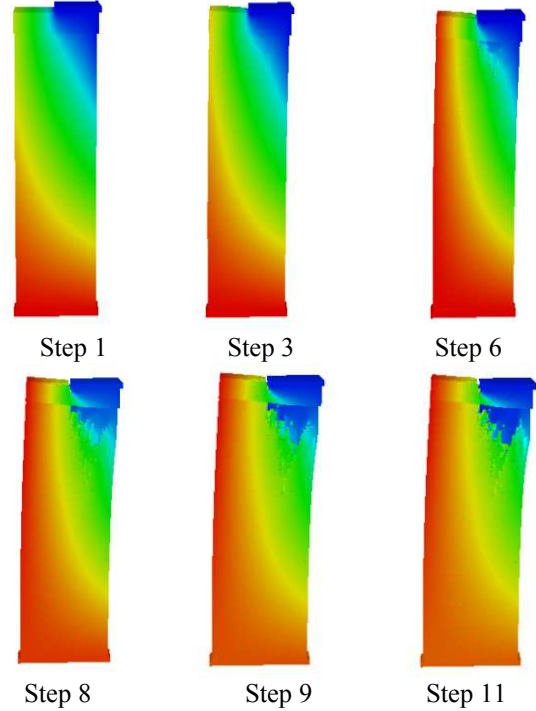


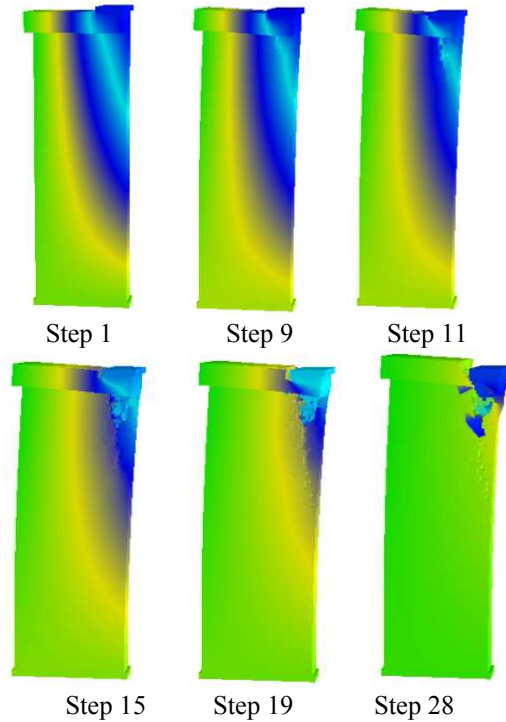
Figure 9: Failure process of  $D_1/D = 1/2$ .

Fig.9 are several important loading steps of a number Mc6 of concrete filled steel tube for 1/2 lap length during whole failure process.

When loading, the maximum stress distribute in a triangular area under the lapped section, the vertex angel of this triangular is smaller than jointing 3/4 length. Increasing loading time, column begins to bend laterally, and the concrete under the junction of lapped surface and free surface begin to destroy; When loading until the 8<sup>th</sup> step, the steel tube has been torn, and the load reaches the maximum simultaneously; Step 9th, the concrete have also new cracks, the part of concrete under the lapped surface has the lateral displacement with the crack propagation, besides the lateral bending of steel tube becomes obvious; Increasing load, the torn steel tube elongates, cracks coalescence, and form a lateral zone.

In the loading process, column shortened is

smaller than  $3/4$  lap length, and column lateral bend is much more obviously than the former.



**Figure 10:** Failure process of  $D_1/D= 1/4$ .

Fig. 10 are several important loading steps of a number Mc6 of concrete filled steel tube for  $3/4$  lap length during whole failure process. A small angel has been turned in the screenshot to observe, because the lateral area is very small: at the beginning, the stress concentration is also a triangular, and the vertex angel is smaller than  $1/2$  lap length, the steel tube reaches the ultimate load when it begins to be torn. The lateral area of lapping portion is quite obvious because of the short lap length. When to be a certain extent in the lateral area (the steel tube expanding to a certain extent), stress has been redistributed, and concentrated in the lateral zone. The lateral bending of the column rebound slightly. Compared with  $3/4$  lap length, the shortening of the  $1/2$  or  $1/4$  lap length column is not clear.

#### 4 CONCLUSION

In this paper, the Realistic Failure Process Analysis (RFPA<sup>3D</sup>) software was used to simulate the concrete-filled rectangular steel tube, following conclusions can be drawn through analysis:

(1)The curves obtained in the numerical simulation about the axial compression process of MC-6 specimens are similar with the experimental curves in reference [7], they can be divided into 4 stages: elastic, elastic-plastic, descent and flattening. According to the simulation results, the first decline period of the load-strain curve is the stripping process of the steel tube and concrete, the speed is associated with the cohesive force between steel tube and concrete, when the load-strain curve go into the flat stage, bearing capacity is associated with steel compressive strength. To improve the steel compressive strength will significantly enhance the residual strength of concrete filled steel tube. Through the analysis of the failure process of the steel tube concrete, the tensile failure is the key factor.

(2)According to observation of this three situations in the eccentric compression numerical simulation, we can conclude the failure characteristics of this load:

1)At beginning of loading, maximum stress concentration at a triangular area under the faying surface .

2)The failure of steel tube start with "torn" in the faying, in the process of loading, the steel tube occurs bending.

3) In the whole loading process, concrete appears two cracks, one is from the lap and free interface along a certain angle obliquely downward, another one is turning midway in the development of the first crack, expanding along the steel tube concrete column section, spitting out to the lap surface to a bottom surface of a lateral area.

4)Lateral zone after forming will be pronounced outward development, at the same time the tube in the formation zone of crack tip will outward bulge, A stress concentration area will be formed when deformation zone developing to a certain extent.

5)Similarly with the axial compression, the loading can also cause steel tube shorten, it is associated with eccentric ratio. The larger eccentric ratio, the smaller column shorten.

#### REFERENCES

- [1] Han, L.H. Concrete-filled steel pipe

structure: theory and practice .Beijing:  
Science Press, 2004.

- [2] Zhong,S.T. Concrete-filled steel pipe structure . Beijing: Tsinghua University Press, 2003.6.
- [3] Cai,S.H. Modern concrete-filled steel pipe structure. Beijing: People Communications Press, 2003.3.
- [4] Zhu,W.C, Tang ,C. A,2002. Numerical simulation on shear fracture process of concrete using mesoscopic mechanical models.Construction and building materials. 16(8):453-463.
- [5] Zhu,W,C,Wang,S.H,Tang,C,A.1999.The concrete three point bending experiment numerical simulation. Journal of northeastern university(natural science), 20(5):533-535.
- [6] Lin,L, Tang,C.A,Yang, J.Y,Wang,S.H, Zhang,Y.A,2008.Three-dimensional numerical simulation of mechanical properties for short short concrete-filled circular steel tubes. Concrete, 20(5):533-535.
- [7] Han,L.H,Yang,Y.F,2001.2001.Study on axial bearing capacity of concrete-filled steel tube columns with rectangular section. China civil engineering Journal, 34(4):22-31.



- tensile apparatus[J]. Machine Design and Research, 2001, 17(3): 68—69(in Chinese))
- [8] 李俊玲, 陈荣, 林玉亮 等. 压拉通用霍普金森杆装置[P]. 中国:101666724,2010 (LI Junling, CHEN Rong, LIN Yuliang, et al. Hopkinson tensile and press general bar apparatus[P]. China: 101666724,2010 (in Chinese))
- [9] 杨鹏飞, 汪洋, 夏源明. 基于 Hopkinson 杆的材料高应变率拉伸实验技术[J]. 实验力学, 2011, 26(6): 674—679 (YANG Pengfei, WANG Yang, XIA Yuanming. Experimental technique of high strain-rate tension based on Hopkinson bar [J]. Journal of Experimental Mechanics, 2011, 26(6): 674—679(in Chinese))

## The Development and Testing Research of Impact Tensile Testing Apparatus

ZOU Guang-ping<sup>1</sup>, CHANG Zhong-liang<sup>1</sup>, WANG Dan<sup>1</sup>, DONG Dan-dan<sup>2</sup>, WANG Xin-zheng<sup>3</sup>

(1. College of Aerospace and Civil Engineering, Harbin Engineering University, Harbin 150001, China;

2. College of Shipbuilding Engineering, Harbin Engineering University, Harbin 150001, China;

3. Northwest Institute of Nuclear Technology, Xi'an 150001, China)

**Abstract:** Since the technology applied in material dynamic experiment is more complicated than that in quasi-static mechanical experiment, so, in order to meet the demands of simulating the process of impact loading at different speeds, the design of experimental device becomes one of the key problems. Especially for the tests of material dynamic tensile properties, there is no uniform standard for impact tensile device. This paper presents a set of double air chamber indirect bar-bar impact tensile testing apparatus designed based on one dimensional elastic stress wave principle. The device adopts a symmetrical arrangement of double air chamber, at the same time, its gas route conversion is realized by a gas converter, which overcome the shortcomings of complex structure, strict sealing demanding existed in current pneumatic impact tensile equipment. The impact tensile properties of 2A12T4 aluminum specimen were tested by this apparatus, and numerical simulation was used for analyzing the stress wave propagation effect in bar system and specimen. The demonstration of design reasonability and experiment reliability of this impact tensile test device is achieved by experimental measurement and numerical analysis.

**Keywords:** impact tensile; split Hopkinson tensile bar; one-dimensional stress wave; double air chamber; numerical simulation